Formulation and Solution of the Classical Seashell Problem.

II. - Tubular Three-Dimensional Seashell Surfaces (*).

C. ILLERT

The Science-Art Centre, Department of Theoretical Conchology
2 Tern Place, Semaphore Park, South Australia 5019, Australia

Summary. — Unlike its predecessor this second paper formulates the problem of seashell geometry entirely in real space E^3, presenting those equations of most use for practical digital computer similations. The mathematics dilates previously mentioned clockspring «wires» (growth trajectories $Y(\phi)$) into tubular spiral surfaces $r(\theta, \phi)$ complete with orthoclinal growth lines and simple periodic corrugations or flares $Q(\theta, \phi)$. It is seen that second-order theory requires a new boundary condition, the famous HLOR growth vector $\dot{r}(\theta, 0)$, which is absent from classical analyses. Thus it is demonstrated that simple periodic surface features, of a kind occurring widely in nature, obey precise Cauchy boundary conditions which may be related to the quantized cyclicities of metabolic, and geophysical, rhythms associated with biological shell growth.

PACS 87.10 – General, theoretical and mathematical biophysics (including logic of biosystems, quantum biology and relevant aspects of thermo-dynamics, information theory, cybernetics and bionics).
PACS 02.70 – Computational techniques.

1. – Introduction.

The classical *first order* model of seashell geometry [1] requires contours of arbitrary shape to sweep along loxodromic real-space trajectories (either conispiral or planispiral), generating what Sir D'Arcy Wentworth-Thompson [2]

---

[1] C. R. ILLERT: *Math. Biosci.*, **63**, 21 (1983).
[2] *a)* Sir D. W. THOMPSON: *On Growth & Form* (C.U.P., Cambridge, 1917). *b) Crescita e forma* (Boringhieri, Torino, 1969).

a)

$$\beta = \frac{1}{2}\pi$$

orthoclines

$$\beta > \frac{1}{2}\pi$$

opisthoclines

$$\beta < \frac{1}{2}\pi$$

prosoclines

b)

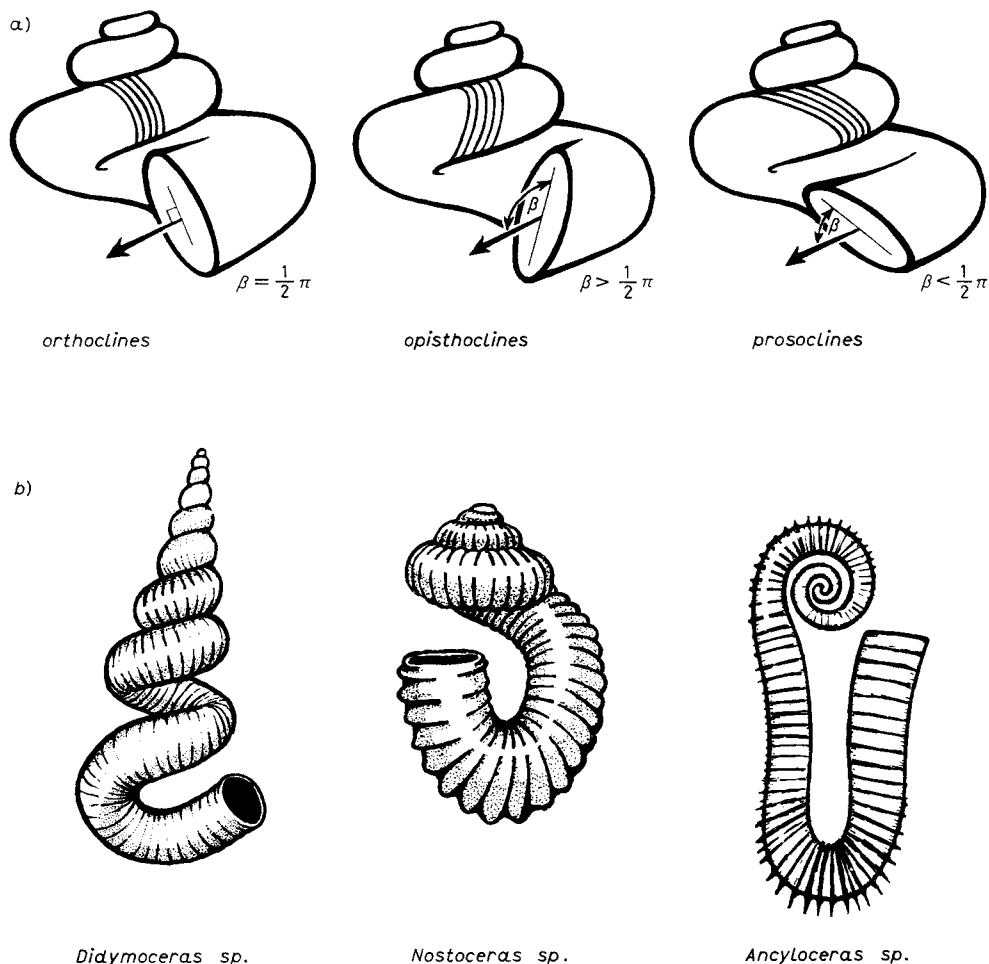*Didymoceras sp.*   *Nostoceras sp.*   *Ancyloceras sp.*

Fig. 1. – *a*) Although these shells all seem identical, they are nevertheless generated quite differently. The inclination of surface growth lines is determined by orientation of the apertural generating curve, relative to the principal growth direction, throughout the course of growth. When the plane of the generating curve is perpendicular to the principal growth direction the shell has *orthoclinal* growth markings; when the angle is obtuse we have *opisthoclines*; and when the angle is acute we have *prosoclinal* growth markings. *b*) Various shells exhibiting approximately orthoclinal growth rings.

called *gnomonic* surfaces. These surfaces are not the solution to any logically complete real-space optimization problem for it is only possible to find Lagrangian energies for the nonaxial real-space coordinates [1]. However, the problem can be formulated in complex space where Schwarz coordinates [3] give

[3] P. J. DAVIS: *The Schwarz Function and its Applications*, Carius Monograph 17, Mathematical Association of America (1974).

rise to a meaningful angular-momentum conservation rule that diagonalizes the Euler equations. Using such complex coordinates, and extending the model to *second order*, gives an elegant logically complete and physically meaningful optimization problem accounting for observed seashell spires and growth trajectories [4].

It only remains to dilate the various growth trajectories («clockspring wires») into the familiar tubular surfaces, but this is not quite as trivial as might first be imagined! Any physically sensible mathematical representation of coiled tubular seashell surfaces (particularly those of second order) must correctly describe the way that surface growth increments orient themselves about sharp corners («apses»). Often growth rings lie in a plane which is oriented perpendicular to the principal growth direction; such rings are said to be *orthoclinal* (see fig. 1). The main purpose of this paper is to demonstrate how to dilate growth trajectories («clockspring wires») into orthoclinally generated tubular surfaces.

More than ever before mathematical models of seashell geometry need to precisely describe the way that growth increments orient themselves about sharp corners. Models of surface colour patterns based upon cellular automata, and the diffusion of chemical substances along the growing edge, have reached an advanced stage. Meinhardt [5] has obtained beautiful and convincing patterns on flat surfaces; it remains to be seen what they look like on properly curved, properly generated, three-dimensional seashell surfaces.

Therefore, starting with first-order growth trajectories in subsect. 2·1, the concept of Frenet coordinates is developed—*i.e.* coordinates which move along with the growing shell aperture instead of remaining arbitrarily anchored to the shell-apex like their *Cartesian* counterparts. Subsection 2·2 relates *Frenet coordinates* to the second-order clockspring trajectories, and a mathematical corollary demonstrates that orthoclinality of surface growth rings is assured by the mutual orthogonality of these moving apertural coordinates. Then various differential and integral models of seashell surfaces are presented in subsect. 3·1. Equation (20) introduces growth vectors about the perimeter of the shell aperture. Owen [6] and others [7] tried to resolve apertural growth vectors into various components, generating a sometimes confusing and contradictory literature on the topic, nevertheless we later refer to Huxley-Lison-Owen-Rudwick (HLOR) growth vectors in honor of these early researchers. The paper concludes attempting to combine the biology and theory of simple surface corrugations and flares—see Vermeij [7c].

[4] C. R. ILLERT: *Nuovo Cimento D*, **9**, 791 (1987).

[5] H. MEINHARDT and M. KLINGER: *J. Theor. Biol.*, **126**, 63 (1987).

[6] *a*) G. OWEN: *Q. J. Microsc. Sci.*, **94**, 57 (1953). *b*) K. M. WILBUR and C. M. YONGE: *Physiology of Mollusca*, part 1 (Academic Press, New York, N. Y., 1964), p. 218.

[7] *a*) M. J. S. RUDWICK: *Geol. Mag.*, **96**, 1 (1959). *b*) L. LISON: *Mem. Inst. R. Nat. Sci. Belg.*, **34**, 1 (1949). *c*) G. J. VERMEIJ: *Forma Functio*, **4**, 319 (1971).

2. – Parametric representation of seashell surfaces.

2˙1. *Cartesian coordinates.* – It was previously demonstrated ([1]) that first-order seashell surfaces can be efficiently described in Cartesian coordinates by parametric equations of the form

$$(1) \qquad r(\theta, \phi) = \exp[\zeta\phi]\, r(\theta, 0) = \exp[\alpha\phi] \begin{bmatrix} \cos\phi & -\sin\phi & 0 \\ \sin\phi & \cos\phi & 0 \\ 0 & 0 & 1 \end{bmatrix} r(\theta, 0),$$

where

$$\zeta = \begin{bmatrix} \alpha & -1 & 0 \\ 1 & \alpha & 0 \\ 0 & 0 & \alpha \end{bmatrix} \quad \text{for some real constant } \alpha,$$

and

$$r : [0, 2\pi] \times [0, \infty) \rightarrow E^3.$$

Read from *right to left* the physical meaning is this: if we take a growth ring (generating curve) coinciding with the shell aperture, rotate it through the angle ϕ (note the rotation matrix), magnify all three of its space dimensions simultaneously by the same scale factor $\exp[\alpha\phi]$, then we have a one-to-one mapping onto the new growth ring at location ϕ. It follows, as D'Arcy Thompson has explained, that all growth rings on «gnomonic» (first order) seashells are similar—retaining their shape throughout growth but changing their absolute size and orientation in space, relative to other pre-existing growth increments, in accordance with eq. (1).

Example. The simplest shell aperture is a circle of radius b, lying entirely in the (x, z)-plane, centred upon the point $Y(0) = (a, 0, -h)$:

$$(2) \qquad r(\theta, 0) = Y(0) + b\cos\theta\,\hat{x} + b\sin\theta\,\hat{z} = \begin{bmatrix} a + b\cos\theta \\ 0 \\ b\sin\theta - h \end{bmatrix},$$

as in fig. 2a). Substituting eq. (2) into eq. (1) gives the following surface equation:

$$(3) \qquad r(\theta, \phi) = Y(\phi) + \exp[\alpha\phi](b\cos\theta\,\hat{e}_2 + b\sin\theta\,\hat{e}_3),$$
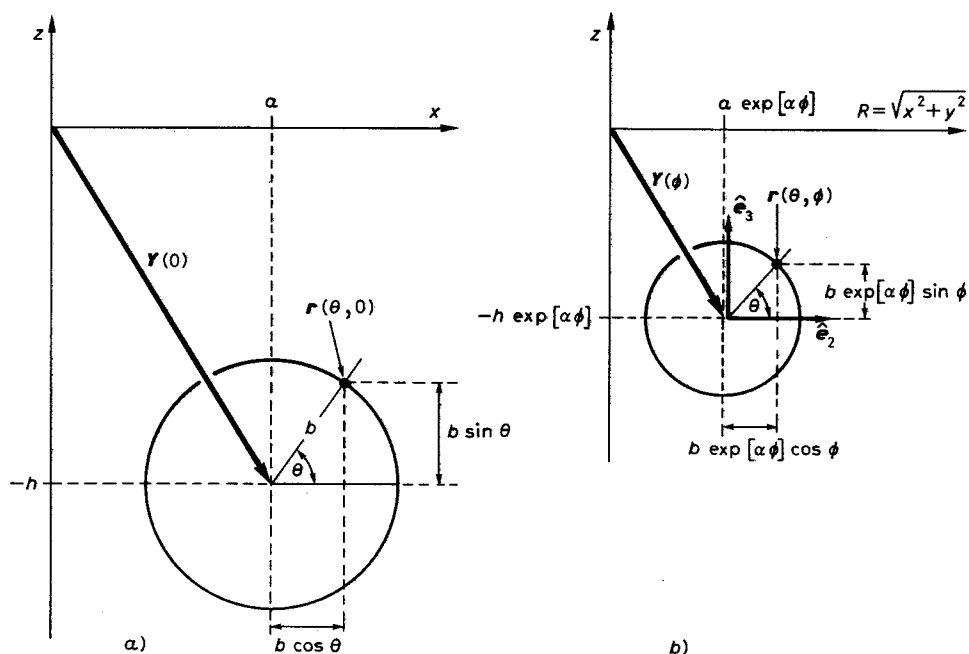
Fig. 2. – a) This circle of radius b, with its centre displaced a distance a along the x-axis and h down the z-axis, represents the shell aperture. It is called the «apertural generating curve» and is described mathematically by eq. (2). b) This diagram shows a generating curve, elsewhere on the shell surface, corresponding to a growth ring subtending an angle ϕ about the axis of symmetry. It is described by eq. (3).
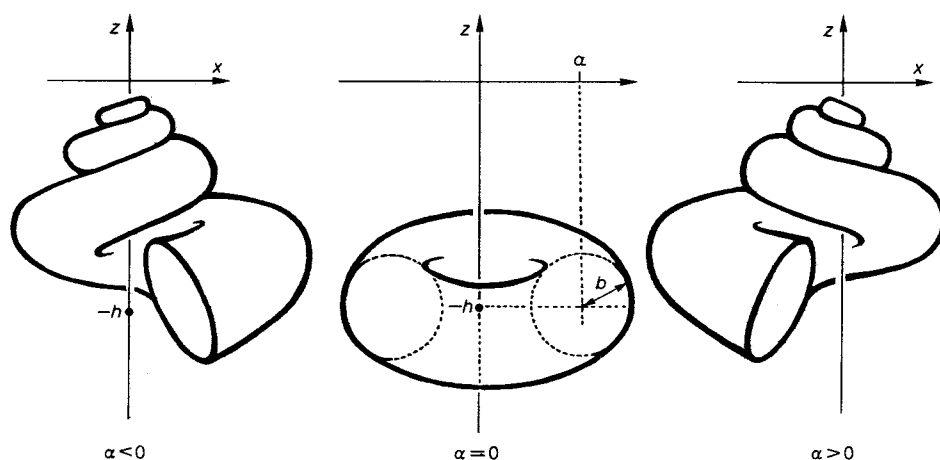

Fig. 3a. – Depending upon the value of α, in eq. (1), surfaces may coil in a left- or right-handed fashion or be figures of revolution.
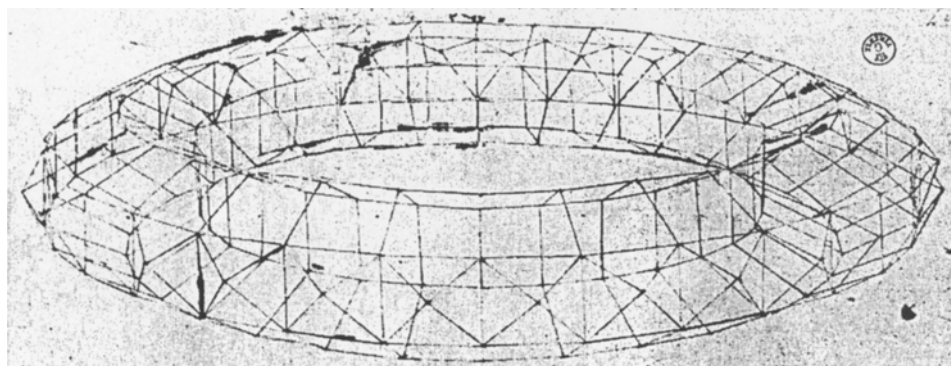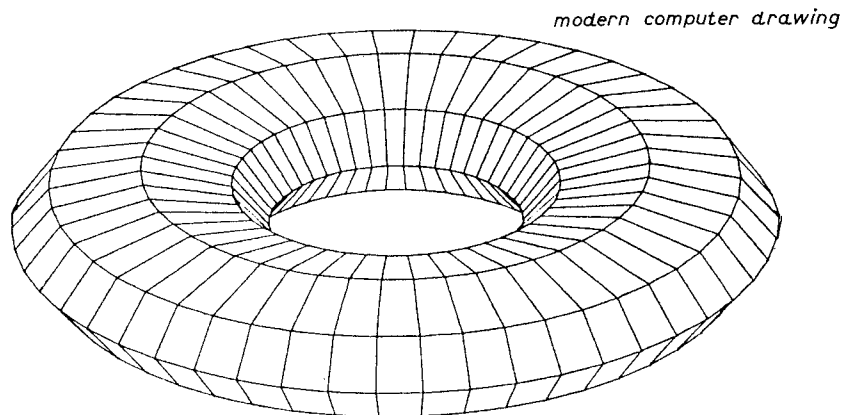
modern computer drawing

Fig. 3b. – This is a drawing of a *mazzocchio*, probably a cartoon for an intarsia wood-inlay panel, by the famous Renaissance master Paolo Uccello. This curved surface, drawn only with ruler and compass, in an age before computers, uses the same incremental construction technique as the molluscal shell. From the Florentine Uffizi archives.

for the unit direction vectors $\hat{e}_2 = \cos\phi\,\hat{x} + \sin\phi\,\hat{y}$ and $\hat{e}_3 = \hat{z}$, and the growth-trajectory $Y(\phi) = \exp[\zeta\phi]\,Y(0)$. Clearly eq. (3) describes a circle of initial radius b, sweeping along the trajectory Y and dilating exponentially but always lying in the $(\hat{e}_2, \hat{e}_3)$-plane (see fig. 2b)). In the special case where $\alpha = 0$ eq. (3) describes a torus of major radius a, and minor radius b, lying parallel to the (x, y)-plane but a distance h below it. For nonzero values of α we have conispiral turbinate tubular surfaces that coil either a *left-* or *right-handed* fashion depending upon whether α is respectively *positive* or *negative*. The height of the shell spire, h, can be set equal to zero for planispiral forms such as Nautilus. See fig. 3 and 7.

Discussion. Although eq. (3) generates the surfaces shown in fig. 3 for differing values of α, the fact is that it generates them wrongly! The shell aperture, eq. (2), and all other growth rings on the surface, slope backward in
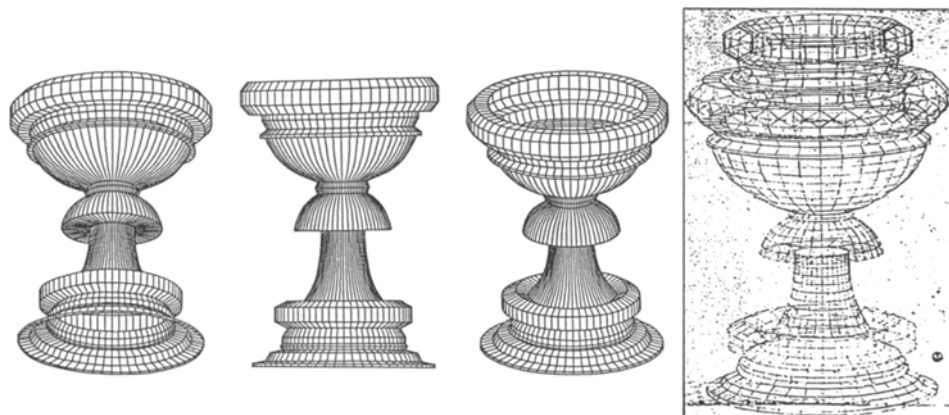
Fig. 3c. – Paolo Uccello's famous chalice, again a figure of revolution, is also a special case satisfying eq. (1) hence also eq. (17); see «Der Mazzocchio des Paolo Uccello» *Jahrbuch der Preussischen Kunstsammlungen* 36, 13-38 plus plates (1915). Importantly the tessellations, on both the *mazzocchio* and the chalice lid, are the simplest possible examples of the molluscan shell corrugations Q (*e.g.* as in fig. 7) mathematically dealt with in appendix B. So, despite the absence of computers, Renaissance Masters pioneered important aspects of curved surface geometry. Figures of revolution were the simplest examples of eq. (13). Sheer physical exhaustion prevented the manual pursuit of this area of graphical analysis and it was not till 1701 that Guido Grandi demonstrated that seashell «gauche» spirals were the orthogonal projection of plane logarithmic spirals onto conical surfaces (see *Nouvelle formation de spirales, Historie de l'academie royale des science*, année 1704, Paris).

biologically unphysical «opisthoclines» (see fig. 1). In the earlier paper[1] a special rotation matrix was introduced to tilt the generating curve forward so that it lay almost in a plane perpendicular to the principal growth direction. But a second smaller rotation, about another axis, was required for exact orthoclinality. These rotation matrices worked on first-order surfaces but the mathematics was messy. It happens that there is a better way to tackle the problem of growth ring inclination. We can use a set of *Frenet coordinates* which move along with the generating curve (the shell aperture) throughout shell growth, constantly changing their orientation along the growth trajectory Y.

2·2. *Frenet coordinates*. – For any specified growth trajectory $Y(\phi):[0, \infty)\to$ $\to E^3$ we can define the three Frenet coordinate unit-vector directions as follows:

$$(4) \qquad \mathbf{e}_1 = \dot{Y}/|\dot{Y}|, \qquad \mathbf{e}_3 = \mathbf{e}_1 \times \ddot{T}/|\mathbf{e}_1 \times \ddot{T}|, \qquad \mathbf{e}_2 = \mathbf{e}_3 \times \mathbf{e}_1/|\mathbf{e}_3 \times \mathbf{e}_1|,$$

where dots denote $\partial/\partial\phi$. See ref. [8].

---

[8] W. F. BRONSVOORT and F. FLOK: *ACM Trans. Graphics*, **4**, 291 (1985).

Fig. 4. – *Frenet coordinates* provide a natural way of describing orthoclinal growth rings on tubular coiled seashell surfaces. Equation (5), for the shell aperture which lies in the $(\mathbf{e}_2, \mathbf{e}_3)$-plane, is a simple vectorial addition; $r = Y - b\cos\theta\,\mathbf{e}_2 + b\sin\theta\,\mathbf{e}_3$.

It is possible to substitute in parametric expressions for Y and its derivatives, multiply out all the cross-products, collect like terms and try to simplify—but it is better not to do it! For one thing, the form of the vectors specified in eq. (4) particularly lends itself to numerical evaluation on modern digital computers (see appendix A). Secondly, although it is possible to do the algebra for the simple conispiral trajectories in subsect. 2`1, eqs. (4) hold true even for the more complicated second-order «clockspring» trajectories given in ref. ([4]), in which case the algebra becomes fierce and one is generally forced to do it numerically.

By analogy with eq. (3), seashell-like surfaces with orthoclinal growth rings may now be written in terms of the new Frenet coordinates as follows:

$$(5) \qquad r(\theta, \phi) = Y(\phi) + \exp[\alpha\phi](- b\cos\theta\,\mathbf{e}_2 + b\sin\theta\,\mathbf{e}_3),$$

and this applies for any second-order «clockspring» trajectory given in ref. ([4]). Reading this equation from right to left, we should imagine a circular generating
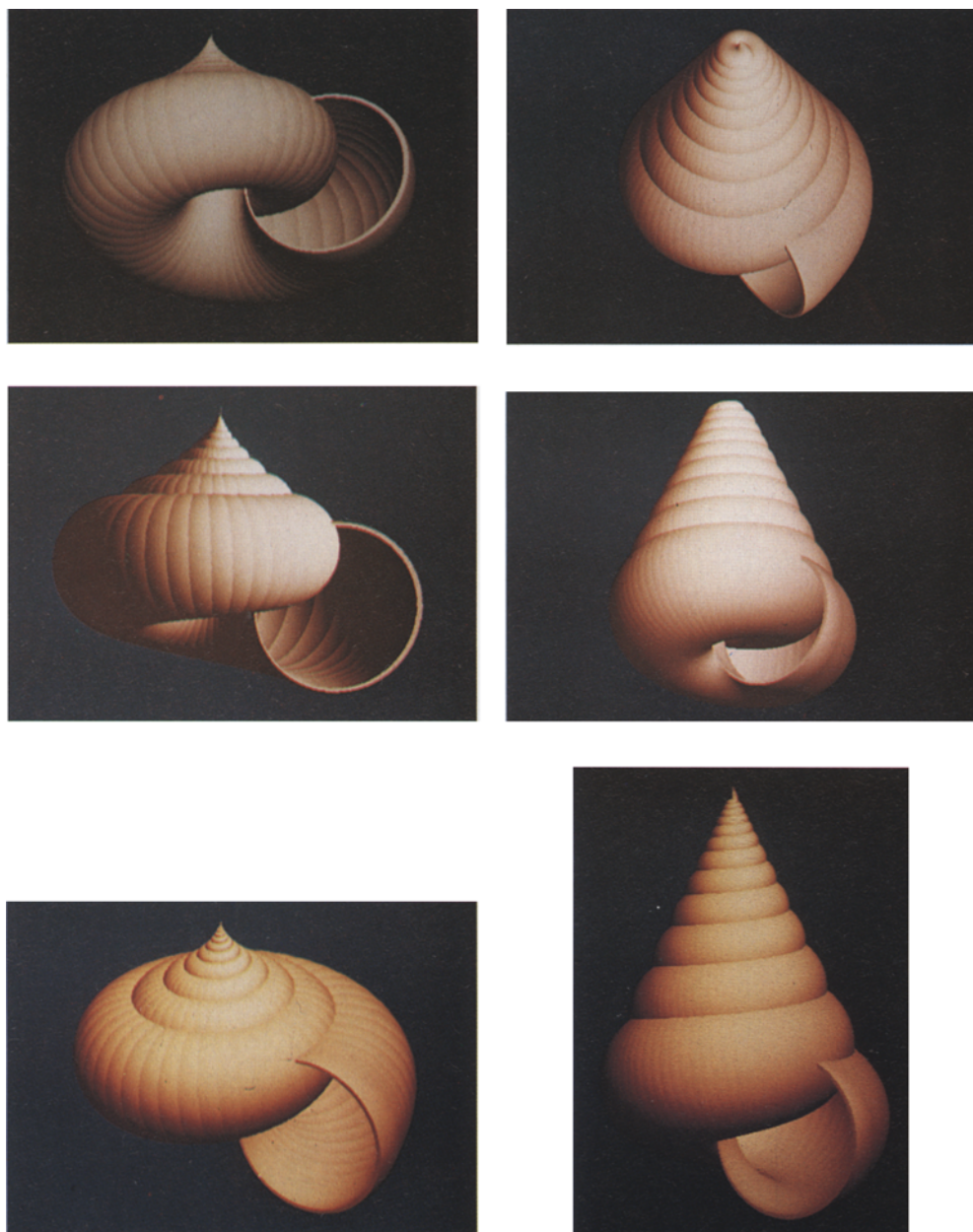
Fig. 5. – Coloured ray-tracing pictures of shells, by Drs. W. F. Bronsvoort, F. Klok, J. van Wijk and K. van Ginkel of the Technische Universiteit Delft, based upon eq. (1), the algorithm of ref. ([8]) and the expanding generating curve (eq. (5)) suggested by the author.

curve of initial radius b, lying in the $(\mathbf{e}_2, \mathbf{e}_3)$-plane (which is always perpendicular to the principal growth direction $\mathbf{e}_1$ as in fig. 4) and dilating exponentially as it translates along the trajectory Y. Other not necessarily exponential scale factors are possible, but it is essential that they act equally on the $\mathbf{e}_2$ and $\mathbf{e}_3$ axes simultaneously otherwise the generating curve would be squashed or deformed throughout the growth process. Bronsvoort *et al.*[8] initially modelled simple helices (using eq. (5) with $\alpha = 0$), overlooking the possibility of dilating generating curves, but have since produced the beatiful images appearing in fig. 5 (using eq. (5) with $\alpha \neq 0$). As the ray-tracing technique paints coloured light over the top of surface markings a simpler less impressive algorithm is supplied in appendix A just to show that all is well in this respect, with growth rings correctly orienting themselves about sharp second-order clockspringlike corners («apses»), and that the Frenet coordinates work beautifully!

Corollary 1. It is a well-known property of Frenet coordinates that

$$(6) \qquad \dot{\mathbf{e}}_1 = \varkappa\,\mathbf{e}_2\,, \qquad \dot{\mathbf{e}}_2 = -\varkappa\,\mathbf{e}_1 - \tau\,\mathbf{e}_3\,, \qquad \dot{\mathbf{e}}_3 = \tau\,\mathbf{e}_2\,,$$

where torsion τ and curvature $\varkappa$ are the two fundamental constants of differential geometry. Of course dots in (6) again denote $\partial/\partial\phi$. See[8].

Corollary 2. The geometrical significance of our orthocline requirement is summarized by the following equation:

$$(7) \qquad (\boldsymbol{r}(\theta, \phi) - \boldsymbol{Y}(\phi)) \cdot \dot{\boldsymbol{Y}}(\phi) = 0\,,$$
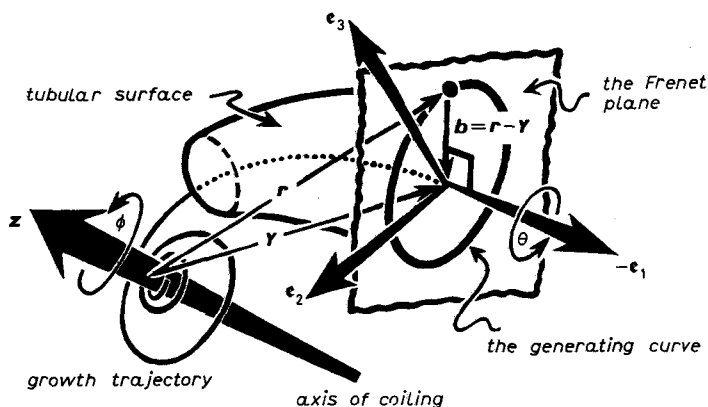

Fig. 6. – This diagram supplies a visual explanation of the significance of the «orthocline constraint» eq. (7). For orthoclines every point about the circumference of the apertural growth ring, hence the vector $\boldsymbol{b}$, always lies in the $(\mathbf{e}_2, \mathbf{e}_3)$-plane which, due to orthogonality of *Frenet coordinates*, is perpendicular to $\mathbf{e}_1$. And the dot product of two perpendicular vectors is zero.

for all $\theta \in [0, 2\pi]$ and any specified value of ϕ. In other words, the vector $\boldsymbol{b} = r - \boldsymbol{Y}$ lies in the plane of the generating curve and is always perpendicular to the principal direction of growth $\dot{\boldsymbol{Y}}$ (see fig. 6).

To check (7) we need only substitute (5) into it. Everything simplifies because $\dot{\boldsymbol{Y}}$ is parallel to $\boldsymbol{e}_1$, and the Frenet vectors are orthogonal:

$$\boldsymbol{e}_2 \cdot \dot{\boldsymbol{Y}} = \boldsymbol{e}_3 \cdot \dot{\boldsymbol{Y}} = 0 .$$

3. – Orthoclinal tubular seashell surfaces.

3`1. *Generalized surface equations.* – From the earlier paper[4] we know that seashells grow along any of a whole range of clockspring trajectories satisfying the second-order real-space differential equation

$$(8) \qquad\qquad \Phi \boldsymbol{Y}(\phi) = \boldsymbol{0} ,$$

where

$$(9) \qquad\qquad \Phi = \left[\frac{\partial^2}{\partial \phi^2} + \Omega \frac{\partial}{\partial \phi} - \zeta^2 - \Omega \zeta \right] ,$$

$$\xi = \begin{bmatrix} \alpha & -1 & 0 \\ 1 & \alpha & 0 \\ 0 & 0 & \alpha \end{bmatrix} \quad \text{and} \quad \Omega = \begin{bmatrix} \lambda & 0 & 0 \\ 0 & \lambda & 0 \\ 0 & 0 & \mu \end{bmatrix} ,$$

for specified real constants α, λ and μ.

But the differential operator (9) can be factorized as follows:

$$(10) \qquad\qquad \Phi = \left[\frac{\partial}{\partial \phi} + \zeta + \Omega \right] \left[\frac{\partial}{\partial \phi} - \zeta \right] ,$$

and the component $[\partial/\partial\phi - \zeta] \boldsymbol{Y} = 0$ ensures the existence of the equiangular «first-order» trajectories $\boldsymbol{Y}(\phi) = \exp[\zeta\phi] \boldsymbol{Y}(0)$ already discussed in eq. (3), as well as the full range of «second order» clockspring curves.

Because of the simple form of eq. (5) it immediately follows that

$$(11) \qquad\qquad \Theta r(\theta, \phi) = \boldsymbol{Y}$$

for the differential operator

$$(12) \qquad\qquad \Theta = \left[\frac{\partial^2}{\partial \theta^2} + 1 \right] .$$

Combining (11) and (8) then gives us a partial differential equation in two variables

$$\Phi\Theta r = \mathbf{0},$$

which can be written in full as

(13) $$\left[\frac{\partial^2}{\partial\phi^2} - \zeta^2 + \Omega\left(\frac{\partial}{\partial\theta^2} - \zeta\right)\right]\left[\frac{\partial^2}{\partial\theta^2} + 1\right] r(\theta, \phi) = \mathbf{0},$$

where $r : [0, 2\pi] \times [0, \infty) \to E^3$ is the parametric Cartesian representation of a simple, smooth, tubular, seashell-like surface which has orthoclinal growthlines everywhere along its clockspring growth trajectory.

But this equation (13) is too specialized. Even if seashell surfaces are of the form (5), the radius b may not be a constant; it often varies with θ and sometimes also with φ. More complicated differential operators can be constructed for such cases but then we lose the elegant simplicity of our formalism. One thing we note regardless of whether or not $b = b(\theta, \phi)$; in the limit as $b \to 0$ in eq. (5) then $r \to T$, ·eq. (11) holds true and eq. (13) simplifies down to eq. (8). This suggests that what we need is an operator which shrinks the tubular surface onto its trajectory—regardless of the function b. If we had such an operator, then we would be able to deal with seashell tubes of complicated cross-section whilst still retaining the simplicity of the operator given in eq. (10).

Corollary 3. From elementary calculus any growth ring, regardless of shape, may be shrunk onto its centre of mass («barycentre») which automatically lies on the trajectory

(14) $$Y(\phi) = \frac{\displaystyle\int_0^{2\pi} r(\theta, \phi)|\partial r(\theta, \phi)/\partial\theta|\,d\theta}{\displaystyle\int_0^{2\pi} |\partial r(\theta, \phi)/\partial\theta|\,d\theta}, \qquad \forall\phi,$$

where the denominator is the growth ring circumference. It is both instructive and reassuring to check this relationship for the simple surfaces specified by eq. (3). In any event we have demonstrated that we do not need a differential operator (12) in order for (11) to hold. The integral operator (14) is better because it even works for noncircular generating curves. Thus a more powerful statement of (13) is possible by combining (14) and (8).

But the shell tube does not always expand exponentially throughout growth. Equation (5) is more often likely to be as follows:

(15) $$r(\theta, \phi) = Y(\phi) + F(\phi)(-b(\theta, \phi)\cos\theta\,\mathbf{e}_2 + b(\theta, \phi)\sin\theta\,\mathbf{e}_3),$$

where $F(\phi) = |Y|$, such that $F(0) = 1$, for growth trajectories defined by (8) and (9). In practice it is convenient to separate eq. (15) into different groups of factors:

$$(16) \qquad \boldsymbol{r}(\theta, \phi) = \boldsymbol{Y}(\phi) + \boldsymbol{P}(\theta, \phi) + \boldsymbol{Q}(\theta, \phi) \equiv \boldsymbol{\Psi}(\theta, \phi) + \boldsymbol{Q}(\theta, \phi),$$

such that

$$(17) \qquad \Phi \, \boldsymbol{\Psi}(\theta, \phi) = 0$$

hence

$$(18) \qquad \Phi \boldsymbol{r}(\theta, \phi) = \Phi \boldsymbol{Q}(\theta, \phi) \equiv \mathfrak{f}(\theta, \phi),$$

where the differentiations inherent in the definition of the function $\mathfrak{f}$ are trivially evaluated by invoking the relations (6).

   Clearly $\boldsymbol{\Psi}$, defined by (16) and (17), describes a smooth featureless expanding tubular surface onto which corrugations $\boldsymbol{Q}$ have been introduced due to the ϕ dependence of the tube «radius» $b(\theta, \phi)$ in (15). Typically we might have $b = b(\theta) \, (1 + 0.3 \sin (30 \phi))$ as in fig. 7 computer simulation. But it is necessary to
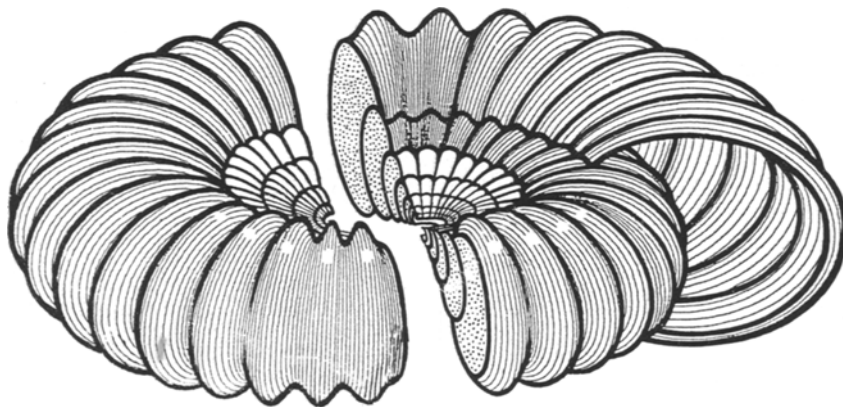

Fig. 7. – Corrugations are introduced onto an otherwise smooth surface: in eq. (15) $b = b_0(1 + 0.3 \sin (30 \phi))$.

precisely know $\boldsymbol{\Psi}$ and $\boldsymbol{Q}$ in (16), before we can claim to have $\boldsymbol{r}$ (the general solution to (18)).

   3´2. *The general solution.* – Taking the *Laplace transform* throughout (18) and rearranging terms gives

$$(19) \qquad \mathfrak{L}\{r\} = \frac{(\mathfrak{T} + \Omega) \boldsymbol{r}(\theta, 0) + \dot{\boldsymbol{r}}(\theta, 0) + \mathfrak{L}\{\mathfrak{f}\}}{\mathfrak{T}^2 + \Omega \mathfrak{T} - \zeta^2 - \Omega \zeta},$$

for $\lambda \neq -2\alpha$ and $\mu \neq -2\alpha$, where $\mathcal{L}\{...\}$ denotes the Laplace transformation, $\mathfrak{T}$ is the diagonal Laplace transform matrix, and matrix «division» merely denotes left-multiplication by the inverse matrix. We note that as both $\mathfrak{T}$ and Ω are diagonal they commute with each other and with ξ, thus the «denominator» can be factored into a difference of two squares $(\mathfrak{T} + (1/2)\Omega)^2 - (\zeta + (1/2)\Omega)^2$ and this enables us to use any standard table of inverse Laplace transforms to derive the result

$$(20) \quad r(\theta, \phi) = \exp\left[-\frac{1}{2}\Omega\phi\right]\left(\cosh(\sigma\phi) + \frac{1}{2}\Omega\sigma^{-1}\sinh(\sigma\phi)\right)r(\theta, 0) +$$

$$+ \exp\left[-\frac{1}{2}\Omega\phi\right]\sigma^{-1}\sinh(\sigma\phi)\dot{r}(\theta, 0) +$$

$$+ \sigma^{-1}\int_0^{\phi} \exp\left[-\frac{1}{2}\Omega(\phi - \psi)\right]\sinh(\sigma(\theta - \psi))\mathfrak{f}(\theta, \psi)\,d\psi,$$

where dots denote $\partial/\partial\phi$ and $\sigma \equiv \zeta + (1/2)\Omega$.

Clearly the convolution integral in (20) can be equal to Q (see appendix B), and the rest equals Ψ, thus (20) can be equivalent to (16). Also the boundary conditions $r(\theta, 0)$ and $\dot{r}(\theta, 0)$ may be trivially obtained from (15) and its derivative, evaluated at $\phi = 0$, with the latter differentiations being accomplished using (6).

But $r(\theta, 0)$ is the vector-valued function, of a single variable, which describes all points about the circumference of the shell aperture. Various authors [9-11] have attempted to correlate the apertural shape with the shell function and habitat. Illert [12], on the other hand, has argued that at least some growth markings on cephalopod shell surfaces may be holographic images of the soft-body mass which produces the shell. Of course the soft-body shape probably is a response to environment, as Linsley suggests, so holographic imagery may simply be a mechanism whereby environment influences the shape of the shell tube's generating curve.

The other vector-valued function $\dot{r}(\theta, 0)$ describes growth velocities at each point about the apertural circumference: it is hereafter called the Huxley-Lison-Owen-Rudwick (HLOR) growth vector at the location $\phi = 0$. In 1932, before vector-valued functions and matrix theory became popular in biological sciences, Huxley in his book *Problems of Relative Growth* tried to resolve apertural growth into components related by a law of «allometry» formulated by Otto Snell

[9] a) R. M. LINSLEY: *Paleobiology*, 3, 196 (1977). b) *Am. Sci.*, 66, 432 (1978). c) *Lethaia*, 14, 224 (1981). See also [10].

[10] C. G. McNAIR et al.: *Lethaia*, 14, 63 (1981).

[11] G. J. VERMEIJ: *Lethaia*, 14, 104 (1981).

[12] C. R. ILLERT: *Bull. Math. Biol.*, 50, 19 (1988).

in 1891 ([13]). He failed and made mistakes. Lison ([7b]) criticized Huxley, the Owen ([6a]) criticized both Lison and Huxley as well as D'Arcy Thompson. This whole area of analysis attained its clearest expression in the recent paper of Vermeij ([7c]) but, unfortunately, they were all wrong. One needs vectors in order to describe nontrivial three-dimensional shapes. In the absence of appropriate mathematical machinery, however, this was probably the best that could be done by them. Of all these workers, perhaps Owen, and in particular Rudwick ([7a]), came closest to dealing with growth velocities about the perimeter of the shell aperture. See also Stasek ([14]).

These workers professed to show how *the form of any accretionary structure can be fully described in terms of the rates of growth operating at different points on the growing edge (of the aperture) during formation of the structure. ... the form of the valve (shell) can be analysed by resolving the rate of growth at each point on the growing edge, at each moment of growth, into component rates acting in different directions* ([7a]). They were in some ways correct in principle, but had no equations that worked in practice.

3˙3. *Boundary conditions and quantized surface corrugations.* – We want eq. (16) to describe a smooth featureless tubular surface Ψ onto which sinusoidal corrugations Q have been added as in fig. 7 and fig. 8a). Appendix B shows that in order for eq. (20) to be equivalent to eq. (16) the following *symmetrical Cauchy boundary conditions* are sufficient:

(21) $$Q(\theta, n\delta) = 0 \quad \text{and} \quad \dot{Q}(\theta, n\delta) = 0\,,$$

for $n = 0, 1, 2, 3, \ldots$ and some fixed finite angle δ.

The first of these two constraints (21) states that the surface grows in similar jumps or corrugations, in separate spurts of macroscopic growth, each of which subtends a finite angle δ. The second of these conditions says that, at the outset of each new spurt of surface growth, the HLOR growth vector starts off with zero slope (*i.e.* parallel to the growth directions about the circumference of the hypothetical bare tube Ψ) before flaring or oscillating in whatever fashion is characteristic of the shell species in question. Essentially the two conditions (21) are a statement of «quantization» of growth energy because, thinking for the moment of a simple sinewave, the shell aperture is required to come to rest (at the end of each growth cycle) on a crest (or a trough) as a maximal (or minimal) ring. It cannot loiter somewhere between because n is an integer.

Sometimes in murexes and strombs the *Cauchy conditions* (21) are satisfied

---

([13]) *a)* O. SNELL: *Arch. Psychiat. Nervkrankh.*, **23**, 436 (1891). *b)* P. F, VERHULST: *Correspondence mathématique etc.*, publié par M. A. Quetelet, Vol. **10** (1838), p. 113.
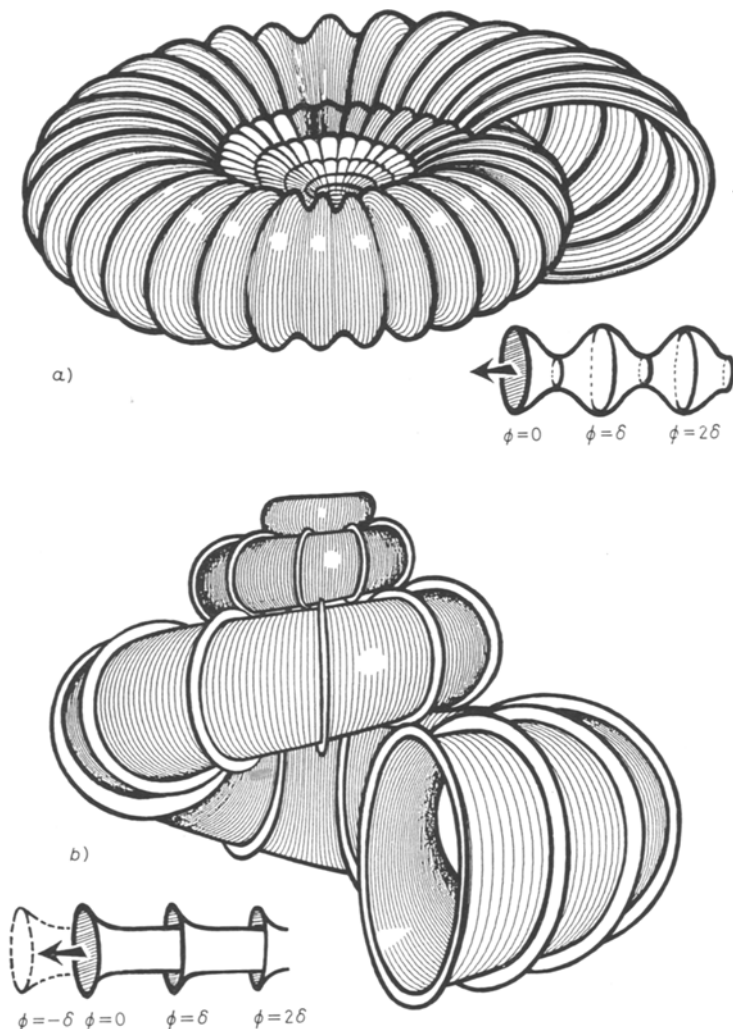([14]) C. R. STASEK: *J. Morphol.*, **112**, 195 (1963).

Fig. 8. – *a*) A computer simulation of a corrugated Ammonite satisfying *symmetrical Cauchy boundary conditions* specified by eqs. (21). The simplified schematic diagram of the shell tube (below right), unwound for the sake of clarity, shows the symmetrical and continuous nature of these conditions (21). *b*) A computer simulation of the «precious Wentletrap shell» *Epitonium scalare* satisfying discontinuous asymmetrical *Cauchy boundary conditions* specified by eqs. (22). Again a simplified schematic diagram of the unwound shell tube (below left) makes clear the physical significance of the boundary conditions.

only in the sense of *asymmetrical* limit, as in fig. 8*b*), where

$$(22) \qquad \lim_{\varepsilon \to 0^+} \dot{\boldsymbol{Q}}(\theta, n\delta - \varepsilon) = 0 \quad \text{but} \quad \lim_{\varepsilon \to 0^+} |\dot{\boldsymbol{Q}}(\theta, n\delta + \varepsilon)| = \infty .$$

These asymmetrical (two-sided) *Cauchy conditions* mean that the growing surface flares outward (attaining infinite slope) toward the end of each segment, but starts growing again with zero slope on the next new segment (see the Wentletrap shell in fig. 8*b*)). In addition to Wentletraps we find that Balers, Clams and even some Cockles (*e.g. Callanaitis disjecta*, Perry) all seem to satisfy the asymmetrical conditions (22) in their own special ways.

Growth quantization is implied because the surface aperture can only come to rest at certain special places on oscillating surfaces which satisfy either (21) or (22); this follows trivially because *n* is an integer. Indeed my aquarium observations of murex shell growth have already demonstrated that growth between these geometrically «allowed» rest locations is intermittent and hurried—indeed a quantized event ([15,16]).

Corroboration has also come from Linsley ([17]) who commented «*the growth of shells from the families Cassidae, Cymatidae, Bursidae and Muricidae indicates that shell growth in these forms is not a continuous event, but occurs in abrupt episodes of growth. During these growth spurts the animal may be vulnerable ... the growth of Cassis apparently represents the most rapid deposition of Aragonite to be found in the phylum mollusca*». My aquarium studies of the Helmet *Cassis bicarinata* ([18]) show that the animal uses its shell aperture to obtain food but can only do so when the current shell segment is completed with a thickened varix; thus either growth is quantized or else the mollusc starves!

But physical explanations like this are seldom unique, molluscan shells grow in quantized segments for as many reasons as there are shells that do it; the one thing they seem to have in common is the transcendent geometrical law summarized either by (21) or (22). One final point is that growth rings are not always orthoclinal. Particularly in bivalved shells, where the two opposing apertures are constrained to meet along a common boundary («commissure line»), it is essential that growth rings be to some extent prosoclinal ([19]). Now that we have the correct clockspring growth trajectories, and a well-defined Frenet coordinate plane, it is a simple matter to model prosoclinal or opisthoclinal growth rings—they are merely inclined at a fixed angle to the orthoclines which this present article has concentrated upon. The Frenet plane provides a reference with respect to which nonorthoclinal growth rings may be defined. Hopefully these equations will provide a basis for more substantial and precise computer modelling in the future.

([15]) C. ILLERT: *Of Sea & Shore*, **12**, 8 (1981).
([16]) G. E. McGINITIE and N. McGINITIE: *The Natural History of Marine Animals* (McGraw Hill, New York. N. Y., 1949). See p. 327-401 and in particular p. 353-356.
([17]) R. M. LINSLEY: *Malacologia*, **20**, 153 (1980).
([18]) C. ILLERT: *Of Sea & Shore*, **11**, 141 (1980).
([19]) E. SAVAZZI: *Lethaia*, **20**, 293 (1987).

* * *

APPENDIX A

The below programme is written in standard AMIGA 500 basic. It runs on an Amiga 500 computer with Commodore 1081 color monitor. For simplicity the hidden-line subroutine has been omitted. It is suggested that the programme be
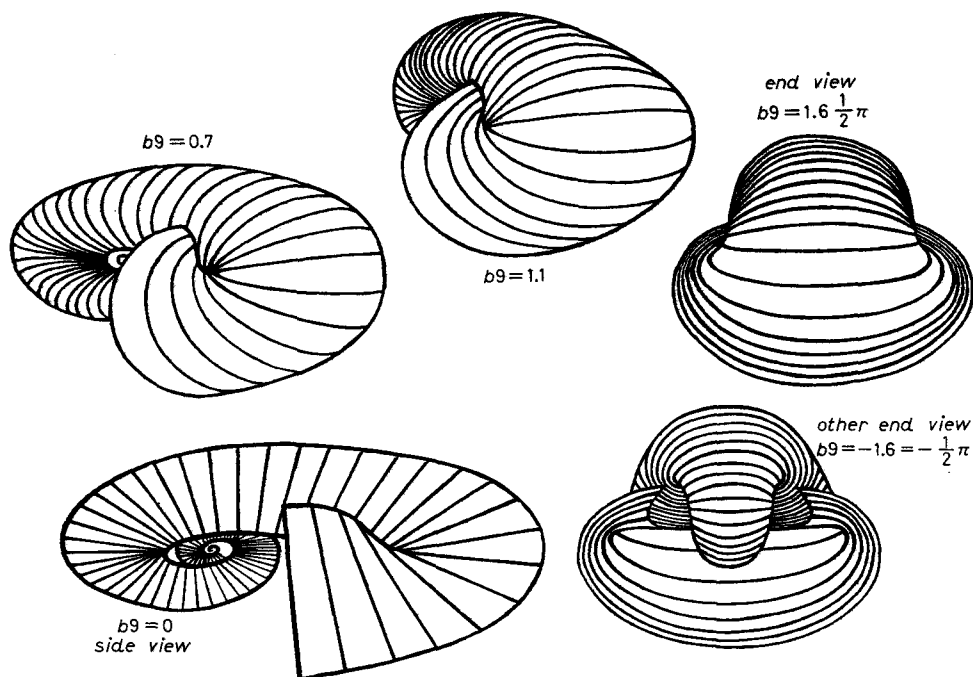

Fig. 9. – *Scaphitid* shell geometry. This is the same shell in each case, generated by the computer programme merely viewed from different angles b9. Observe how the growth rings orient themselves orthoclinally as the shell tube grows round the sharp apse.

tried first with b9 = 0, then using whatever other values one desires. The shell itself is a Cretaceous Ammonite called *Scaphites* (see fig. 9). It is a clockspring of the first kind. In the programme $\alpha = a1$, $\lambda = l$, $\phi = i$, $\theta = j$. The picture screen is assumed to be 600 pixels by 180 pixels and upsidedown.

```
b9=0
b=.45
a1=.5
l=-.7
pi=3.1418
FOR i=-10 TO -1.88 STEP pi/30.01
    e=EXP(a1*i)
    e2=EXP(-i*(a1+l))
    c=COS(i)
    s=SIN(i)
    p1=.5*(e+e2)*c
    p2=.5*(e-e2)*s
    p3=0
    q1=.5*(a1*e-(a1+l)*e2)*c-.5*(e+e2)*s
    q2=.5*(a1*e+(a1+l)*e2)*s+.5*(e-e2)*c
    q3=0
    r1=.5*((a1^2-1)*e+((a1+l)^2-1)*e2)*c-(a1*e-(a1+l)*e2)*s
    r2=(a1*e+(a1+l)*e2)*c+.5*((a1^2-1)*e-((a1+l)^2-1)*e2)*s
    r3=0
    l1=q1
    l2=q2
    l3=q3
    n1=q2*r3-q3*r2
    n2=q3*r1-q1*r3
    n3=q1*r2-q2*r1
    m1=n2*l3-n3*l2
    m2=n3*l1-n1*l3
    m3=n1*l2-n2*l1
    u=SQR(l1^2+l2^2+l3^2)
    v=SQR(m1^2+m2^2+m3^2)
    w=SQR(n1^2+n2^2+n3^2)
    u1=l1/u
    u2=l2/u
    u3=l3/u
    v1=m1/v
    v2=m2/v
    v3=m3/v
    w1=n1/w
    w2=n2/w
    w3=n3/w
    FOR j=0 TO 2*pi STEP pi/10.01
        c4=COS(j)
        s4=SIN(j)
        e5=.5*(e+e2)
        x=p1+e5*b*(-c4*v1+s4*w1)
        y=p2+e5*b*(-c4*v2+s4*w2)
        z=p3+e5*b*(-c4*v3+s4*w3)
        x=x*COS(b9)-z*SIN(b9)
        z=x*SIN(b9)+z*COS(b9)
        x1=(x+.65)*600
        y1=(y+.65)*180
        GOSUB 520
    NEXT j
NEXT i
END

520 y1=200-y1
    IF NOT j=0 THEN
        LINE (x0,y0)-(x1,y1)
    END IF
    x0=x1
    y0=y1
RETURN
```

APPENDIX B

Theorem:

$$\boldsymbol{Q}(\theta,\phi) = \sigma^{-1} \int_0^\phi \exp\left[-\frac{1}{2}\Omega(\phi-\psi)\right] \sinh(\sigma(\phi-\psi)) \left[\frac{\partial}{\partial\psi}+\zeta+\Omega\right]\left[\frac{\partial}{\partial\psi}-\zeta\right]\boldsymbol{Q}(\theta,\psi)\,\mathrm{d}\psi,$$

if

$$Q(\theta, n\delta) = 0$$

and

$$\dot{Q}(\theta, n\delta) = 0 \,,$$

for some fixed angle δ and $n = 0, 1, 2, \dots$. These *Cauchy boundary conditions* being jointly sufficient but not strictly necessary.

Proof. Using the result given in appendix C we can «nest» the factorized differential operator in order to implement an obvious two-step integration by parts. Alternately we can Laplace transform the whole convolution to obtain the result

$$(\mathfrak{T}^2 - \zeta^2 + \Omega(\mathfrak{T} - \zeta))^{-1}(\mathfrak{T} + \Omega)Q(\theta, 0) + \dot{Q}(\theta, 0)) = 0 \,.$$

And this is required to hold for all real values of the *Laplace transform* matrix $\mathfrak{T}$. Clearly one way that this can be true is if the above *Cauchy conditions* hold.

APPENDIX C

An alternative derivation of the Cauchy conditions.

Readers without a background in integral transform theory would not have understood the derivation of the *Cauchy conditions* (21) from appendix B. Fortunately an alternative proof can be given. For any 3×3 constant matrix W, the differential operator $D = \partial/\partial\psi$, and any corrugation function $Q: [0, 2\pi] \times \times [0, \infty) \to E^3$ we may repeatedly use the fact that

$$[D - W]Q = \exp[W\psi]D\{\exp[-W\psi]Q\}$$

in order to obtain the result

$$[D - \zeta + \Omega][D - \zeta]Q = \exp[-(\zeta + \Omega)\psi]D\{\exp[(2\zeta + \Omega)\psi]D(\exp[-\zeta\psi]Q)\} \,.$$

Substituting this into the integrand enables us to integrate by parts, in a now obvious two-step process, in order to obtain the constraints (21).

● RIASSUNTO

A differenza del precedente quest'articolo formula il problema della geometria delle conchiglie completamente in spazio reale E^3, quindi presentando quelle equazioni piú utili nella simulazione pratica del computer numerico. In questa discussione i «fili» elastici a molla d'orologio (traiettorie di crescita $Y(\not\varphi)$) sono dilatati quindi diventano superfici a spirale tubolare $r(\theta, \not\varphi)$ e completi di anelli ortoclinati (orientati perpendicolari alla direzione di crescita) e ondule $Q(\theta, \not\varphi)$ periodiche semplici. Si vede che nella teoria di

secondo ordine è richiesta una condizione di confine nuova, il ben conosciuto HLOR vettore di crescita $\dot{r}(\theta, \dot{\phi})$, che è assente nell'analisi classica. Quindi è dimostrato che le caratteristiche periodiche semplici delle superfici, simili a quelle molto frequenti in natura, obbediscono a precise condizioni di confine di Cauchy le quali possono essere collegate con ciclicità pulsanti di ritmi metabolici e geofisici associati con la crescita biologica delle conchiglie.

Цилиндрические трехмерные поверхности морских раковин.

Резюме (*). — В отличие от первой части в этой статье формулируется проблема геометрии морской раковины полностью в реальном пространстве E^3, с целью получения уравнений, удобных для практического компьютерного моделирования. Математический аппарат позволяет растянуть ранее предложенные растущие траектории $T(\dot{\phi})$ в цилиндрические поверхности $r(\theta, \dot{\phi})$, которые заканчиваются ортоклинными растущими линиями и простыми периодическими складками или раструбами $Q(\theta, \dot{\phi})$. Отмечается, что теория второго порядка требует нового граничного условия, известного HLOR вектора $\dot{r}(\theta, 0)$, который отсутствует в классическом анализе. Показывается, что характеристики простых периодических поверхностей, широко встречающихся в природе, подчиняются граничным условиям Коши, которые могут быть связаны с квантованными цикличностями метаболических и геофизических ритмов, связанных с ростом биологических раковин.

(*)   *Переведено редакцией.*